Proceedings of the 7th GACM Colloquium on Computational Mechanics for Young Scientists from Academia and Industry October 11-13, 2017 in Stuttgart, Germany

Transient aeroelastic simulations of wind turbines with composite blades.

Gilberto Santo[1]*, Mathijs Peeters[2], Wim Van Paepegem[2] and Joris Degroote[1]

Micro Abstract
A fluid-structure interaction model is employed to numerically investigate the interaction of wind flow and blade structures of a horizontal axis wind turbine. On the fluid side, the atmospheric boundary layer is included and sliding interfaces are adopted to handle the rotation of the rotor. On the structural side, a detailed model of each blade composite structure is used. The two models are coupled in a transient simulation where stresses, loads and deformations of the blades are monitored.

[1]Dpt. of Flow, Heat and Combustion Mechanics, Ghent University, Gent, Belgium
[2]Dpt. of Materials, Textiles and Chemical Engineering, Ghent University, Gent, Belgium
***Corresponding author**: gilberto.santo@ugent.be

1 1 Introduction

Since the dimensions of horizontal axis wind rotor tend to increase, the slenderness of their blades is also sensibly increasing. The deflection of the blades due to the wind load can reach peaks of 15% [1]. This leads to a fully coupled fluid-structure interaction (FSI) problem where the wind flow and the flexible blades influence each other and continuously interact. This work aims at simulating the FSI on a full scale horizontal axis wind turbine employing accurate computational fluid dynamics (CFD) and computational structural mechanics (CSM) models. The atmospheric boundary layer (ABL) is taken into account in detail. The resulting oscillating loads and stresses on each blade are analyzed. On the structural side, a complete and accurate model reproducing the complex composite nature of each blade is employed. The implicit coupling between the flow and the structural models is guaranteed by the in-house code Tango, resulting in a segregated approach [2].

2 1 CFD model

Given the relative motion of the modeled wind turbine, two different domains (a rotating and a stationary one) are adopted, separated by sliding interfaces. The layout of the complete mesh and the imposed boundary conditions are shown in Fig. 1. The rotor, whose radius R is 50 m,

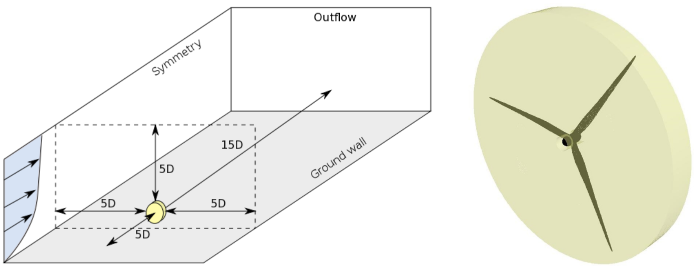

Figure 1. (left) Layout of the simulations and (right) detail of the rotating domain

is embedded in the rotating cylindrically-shaped domain (marked in yellow in Fig. 1, which has a length of 12 m and a radius of 52 m. The mesh is fully hexahedral and obtained by means of multi-block strategy. The rotating domain consists of 3 M cells, while the stationary one of 10 M cells.

The turbulence model is chosen to be the $k-\varepsilon$ (unsteady RANS) model. The atmospheric boundary layer inlet conditions first proposed by Richard and Hoxey [5] are employed in order to replicate the neutral ABL conditions in the numerical domain, with friction velocity $u^* = 0.79196\ m/s$ and aerodynamic roughness length $y_0 = 0.5\ m$. The modified wall functions proposed by Parente and Benocci [3] are employed on the ground wall to correctly preserve the ABL profiles throughout the domain.

3 1 The CSM model

The analyzed blade is entirely made of composite material, with a total weight exceeding 9 *tons*. Only shell elements are employed and composite layups are defined to reproduce the composite layering. The elements are positioned on the outer mold layer (OML) with material offset towards the inside. Different layups are assigned to different regions of the structure, mimicking its real composition. Each layup is composed of a varying number of plies (up to 127). For each ply a material and a thickness are assigned, together with the necessary orientation to fully define the characteristics of layers made of anisotropic materials. The shear webs and the shear caps are modeled using the same strategy. The mesh is created according to the process outlined and discussed in [4]. Following this procedure, a mesh composed of 64000 three-dimensional shell elements is obtained.

4 1 Coupling

The two outlined models are coupled by an in-house code named Tango [2]. The Gauss-Seidel coupling algorithm is chosen in order to enforce equilibrium at the fluid-structure interface within every time step. The displacements prescribed by the CSM model are applied on the CFD mesh where the diffusion method based on boundary distance is chosen to deform only the rotating domain mesh.

5 1 Results

The results of a fully coupled FSI simulation are compared with the ones coming from a purely CFD simulation, thus considering rigid blades. In both cases the rotor spins at 1.3 rad/s and a full revolution is simulated in 120 time steps. The logics illustrated in Fig. 2 will be used to define the azimuth angle of each blade and the sign of the radial and tangential forces and velocities.

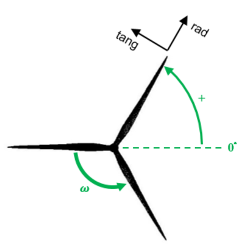

Figure 2. Definition of the blade azimuth angle and components of forces and velocities.

Furthermore, as usually done, the torque (T) and the forces (F) acting on the blades are made non-dimensional by means of the formula: $c_T = T/(\frac{1}{2}\rho v^2 AR)$ and $c_F = F/(\frac{1}{2}\rho v^2 A)$ where v is the wind velocity at the hub height (10 m/s), ρ the air density and A is the frontal area of the rotor. The velocity distribution induced by the ABL leads to higher angles of attack on the blade span when the it points upwards (positive azimuth angles) and lower angles of attack when it points downwards (negative azimuth angle). As a result, the torque contribution follows the same trend, as illustrated by Fig 3.

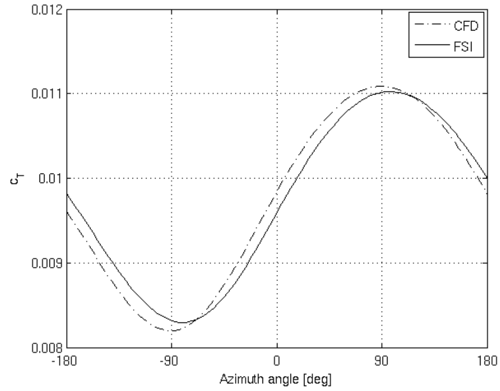

Figure 3. Single blade contribution to the torque as a function of the azimuth angle.

No difference is reported in the average value of the single blade contribution to the torque (about 0.01) while a reduction in the peak-to-peak amplitude of the oscillation (-3.8%) is visible in the FSI case. A delay is also reported in the FSI case. These differences are linked to the axial oscillation of the tip in the FSI case, showed in Fig. 4 in terms of axial displacement and axial velocity. A positive tip axial velocity leads to a reduction of the angle of attack at the tip

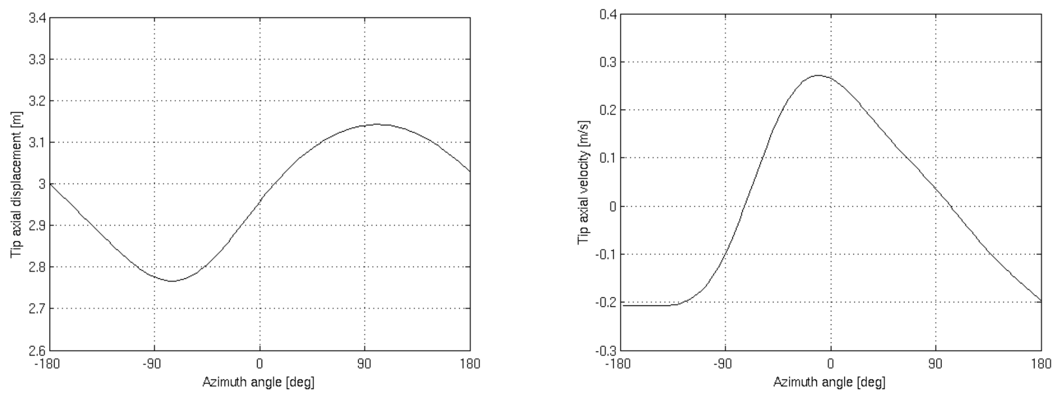

Figure 4. (left) Tip axial displacement and (right) axial velocity in the FSI case.

and, consequently, to a local decrease of the performance. Similarly, a negative tip axial velocity leads to an increase of the tip angle of attack and thus to an increase in the local performance. A comparison of Fig. 4 and Fig. 3 shows that when the tip speed is positive, the FSI torque is lower than the CFD torque, confirming the reasoning just outlined. Fig. 5 compares the total radial force induced by the wind load on the blade in the CFD and FSI cases: it can be seen that the radial aerodynamic force is centrifugal in the CFD case but becomes centripetal in the FSI case.

Focusing on the internal stresses, most of the load acting on the blade is counteracted by its inner shear webs, which are always solicited by bending moment during the revolution. In particular, the pressure side experiences traction longitudinal stress, while the suction side is subject to compression stress. Fig. 6 monitors the longitudinal stresses in the maximal traction and maximal compression points in the shear webs.

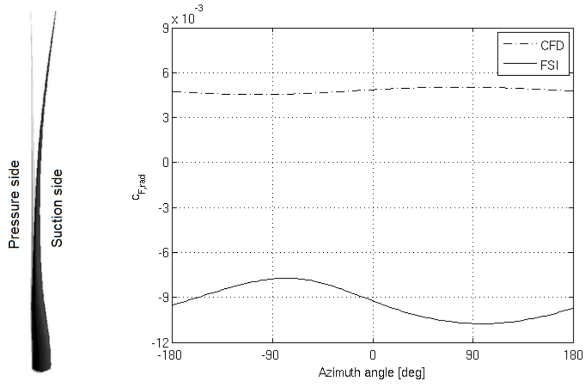

Figure 5. (left) Deformed blade on top of undeformed one and (right) radial aerodynamic force on the blade.

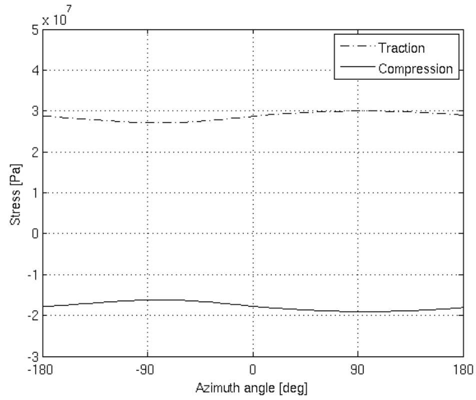

Figure 6. Stress evolution in the maximal traction and maximal compression points of the shear webs.

6 1 Conclusions

The FSI model described was successfully used to investigate the mutual interaction of wind flow and structural response of a modern horizontal axis wind turbine. The effect of the ABL was also highlighted in both CFD and FSI cases. A noticeable effect of the tip deflection on the performance of the turbine was addressed.

1 References

[1] Y. Bazilevs, M. Hsu, J. Kiendl, R. Wüchner, and K. Bletzinger. 3D simulation of wind turbine rotors at full scale. Part II: Fluid-structure interaction modeling with composite blades. *Int. journal for numerical methods in fluids*, Vol. 65:p. 236–253, 2011.

[2] J. Degroote. Partitioned simulation of fluid-structure interaction: Coupling black-box solvers with quasi-Newton techniques. *Archives of computational methods in engineering*, Vol. 20(3):p. 185–238, 2013.

[3] A. Parente, C. Gorlé, C. van Beeck, and A. Benocci. Improved k–epsilon model and wall function formulation for the RANS simulation of ABL flows. *Journal of wind engineering and industrial aerodynamics*, Vol. 99:p. 267–278, 2011.

[4] M. Peeters and V. P. W. Development of automated high fidelity finite element models for large wind turbine blades. In *16th European Conference on Composite Materials: 22-26 June 2014, Sevilla, Spain.*, Sevilla, 2014.

[5] P. Richard and R. Hoxey. Appropriate boundary conditions for computational wind engineering models using the k-epsilon turbulence model. *Journal of wind engineering and industrial aerodynamics*, Vol. 46:p. 145–153, 1993.